Experimental and numerical investigation of the fire performance of densified spruce wood

Tran Trong Tuan[(1)]

Abstract

This paper presents experimental and numerical investigations to assess the relative fire structural resistance of thermo-mechanically compressed (or densified) spruce wood. First of all, both compressed and uncompressed spruce samples of dimensions of 100 mm x 100 mm x 19 mm have been subjected to fire in a cone calorimeter under 20 kW/m2 and 75 kW/m^2. Finally, a predictive finite element model based on three-step multi-reactions of pyrolysis is proposed for the thermal transfer and degradation analyses of timber material. The simulated thermal profiles, the mass loss as well as the charring depths were compared to the experimented results showing a fairly good agreement.

Key words: *Wood, Fire Performance, Finite Element Method, Pyrolysis, Thermal Transfer*

(1) PhD. Lecturer, faculty of civil engineering, Hanoi Architectural University, Email: tuan87kta@gmail.com

Date of receipt: 15/4/2022
Editing date: 6/5/2022
Post approval date: 5/9/2022

1. Introduction

Fire resistance should be understood as the characteristic times involved in the degradation, burning and loss of density and mechanical properties of the material. Among other timber species, spruce timber is known for its lower thermo-physical properties (thermal conductivity, specific heat and density) thanks to its porosity level. However, information on the thermo-physical properties of compressed spruce timber is not available. In fact, the objective of the thermomechanical compression process is to increase the density of spruce timber by reducing as much as possible its porosity, which in turn can greatly affect the thermal conduction.

It has been found that the densification process increases the fire performance of wood material by modifying the thermal properties [1–2], including heat release rate and flammability. Gan et al. [3] presented a study showing how delignification and densification of wood can substantially improve the fire-retardant properties of wood materials. Yue et al. [4] combined resin impregnation and densification of Chinese fir to improve its combustion performance. Chen et al. [5] combined delignification, bentonite impregnation, and densification of wood to enhance flame-retardancy of wood.

Pyrolysis is a crucial process to understand the fire behavior of wood [6–8]. In recent years, pyrolysis modeling is extensively used to predict the thermal degradation of polymers in general and wood in particular. Several numerical pyrolysis models have been formulated for wood including basic and more detailed chemical schemes to represent the transformation of the virgin components of wood, namely hemicellulose, cellulose, and lignin. Readers can referr to [1–16] for a better reading on the pyrolysis chemical schemes and related modeling aspects.

In this paper, the heat transfer and thermal degradation of both compressed and uncompressed spruce have been studied experimentally and compared. The pyrolysis process suggested by Blasi et al. [17], was modified and extended to a three-steps multi-reactions pyrolysis finite element model to deal with the thermal behavior of wet wood under fire conditions. The developed pyrolysis finite element (FE) model was calibrated with regard to the experimental database and used to simulate the thermal behavior of uncompressed and compressed wooden plates under fire conditions.

2. Fire tests under a cone calorimeter

2.1. Materials

Spruce timber plates without visible defects, either compressed or uncompressed, having the dimensions of 100mm x 100mm x 19mm were used in this study (Figure 1). The initial density of the uncompressed spruce plates was 449 kg/m^3 (±3%). The compressed wood plates were obtained by thermomechanical compression of spruce blocks (cut from the same wood as for the uncompressed plates) in the radial direction [18] up to a compression ratio (CR) of 68% (the CR is defined as the ratio between the final and initial thickness). For a better reading of the compression process, readers can referr to [18]. Thanks to the thermomechanical compression process, the mean density of the spruce plates was increased from 449 kg/m^3 to 1210 kg/m^3 (±1.4%).

2.2. Experimental set-up

Experiments on thermal decomposition of both compressed and uncompressed spruce were undertaken using a cone calorimeter (Figure 2) using the samples depicted in Figure 1 with dimensions of 100mm x 100mm and 19mm thick, with moisture content (MC) ranging from 7 to 8%. All the samples were heated on one side using two different uniform heat fluxes, namely 20kW/m^2 and 75kW/m^2, with a potential of maximal temperatures at the exposed surfaces of 600°C and 850°C, respectively. The unexposed surfaces (one opposite and four lateral surfaces) were protected from direct heating to allow exchange with the room temperature. K-type thermocouples were placed on both the exposed and the unexposed surfaces to record the temperature rise during the thermal decomposition. The mass of samples was continuously recorded using a precise electronic balance every one second. In addition, an infrared camera was used to control the distribution of the heat flux on the exposed surface. The tests were carried out according to the standard ISO 5660-1.

2.3. Experimental results

Figures 3 and 4 display the mean experimental mass loss curves over the fire exposure time under 20kW/m^2 and 75kW/m^2 heat fluxes, respectively, for both the uncompressed and compressed spruce samples. It can be observed from Figure 3 that both the uncompressed and compressed samples exhibit a similar plateau-like mass loss up to about 300°C, which corresponds to the isotherm point of the pyrolysis. The beginning of this plateau corresponds to the drying stage up to about 100°C.

Beyond the temperature level of 300°C, corresponding to about 5 min exposure time to fire, the thermal decomposition of both uncompressed and compressed samples starts but the uncompressed samples pyrolyzed very quickly as compared to the compressed samples. However, in the case of heat flux of 75kW/m^2 (Figure 4), both uncompressed and compressed samples do not exhibit the plateau-like mass loss, and the thermal decomposition of both starts from the beginning of heating, and no obvious drying process was observed at this heating level (75kW/m^2) because probably, this has occurred very quickly. This result is coherent with that reported in [19]. Moreover, it can be clearly seen that the pyrolysis (charring rate) of the compressed samples is very slow by comparison to the uncompressed samples.

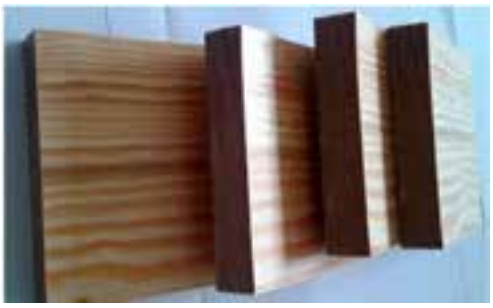

(a) Uncompressed samples

(b) 68% compressed samples

Figure 1: Typical studied spruce timber plates

Furthermore, the experimental charring layers for both uncompressed and compressed samples are depicted in Figure 5. The experimental observation of the charring depths confirms the results depicted in Figures 3 and 4. It can, therefore, be concluded that the compressed samples exhibit low charring rate than the uncompressed ones.

3. Numerical simulation

3.1. Finite element modeling

A finite element model for the thermal behaviour (pyrolysis) of timber under fire based on three-steps multi-reaction kinetics is proposed. The model is inspired by the three-steps kinetic model proposed by Blasi et al. [17] to analyze the thermal decomposition of wood. That model states that dry wood is composed of three pseudo-components A_1, A_2, and A_3, each of them corresponds to specific kinetic law and a mass fraction α_1, α_2, and α_3, respectively [17].

The general flowchart of the proposed three-steps pyrolysis model is given in Figure 6, including the drying

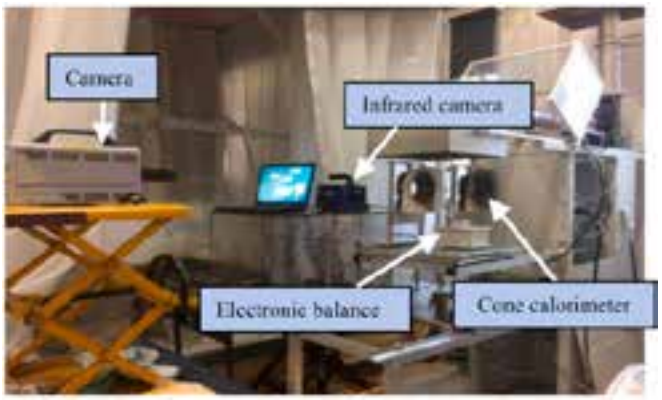

Figure 2: Experimental set-up for cone calorimeter test

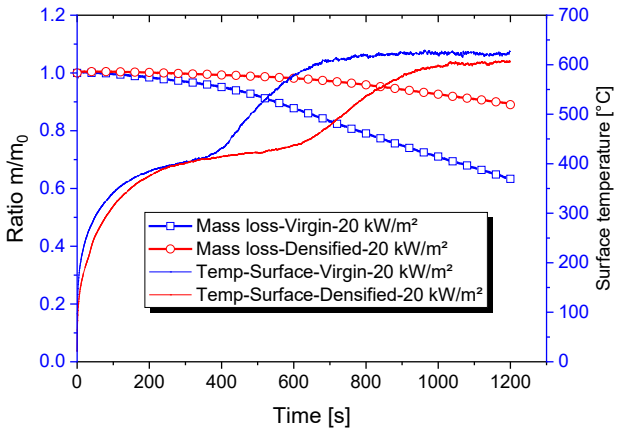

Figure 3: Experimental mass loss under exposure to 20 kW/m^2 heat flux

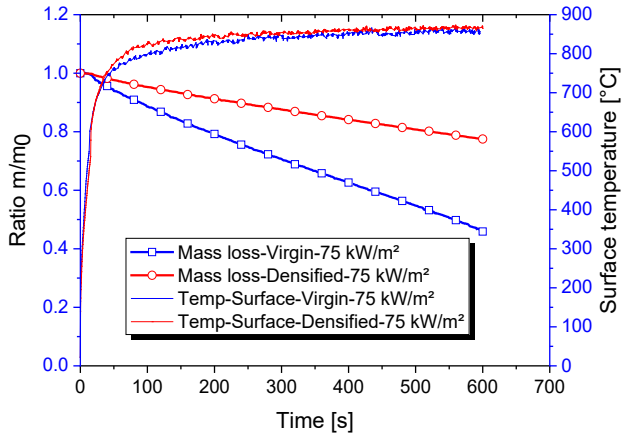

Figure 4: Experimental mass loss under exposure to 75 kW/m² heat flux

process. As shown in Figure 6, the kinetic mechanisms involved in the three parallel decompositions of the pseudo-components A_1, A_2, and A_3 are associated with the rate constants of reactions k_1, k_2, and k_3. By assuming that the kinetic is described by first-order laws for the three reactions, the mass balance of the wet solid and associated components can be expressed as follows:

$$\frac{dm_l}{dt} = -k_v.m_l \quad (1)$$

$$\frac{dm_{A1}}{dt} = -k_1.m_{A1} \quad (2)$$

$$\frac{dm_{A2}}{dt} = -k_2.m_{A2} \quad (3)$$

$$\frac{dm_{A3}}{dt} = -k_3.m_{A3} \quad (4)$$

Eqs. (1) to (4) show that the mass of the sample during the pyrolysis at a fixed temperature in an inert atmosphere depends on six parameters (α_1, α_2, α_3, k_1, k_2, and k_3), which are defined based on experimental data, including inverse approach analysis using the gravimetric test data.

The energy conservation equation for the pyrolysis of the wet wood was adapted from the one-dimensional model by Shen et al. [20] and modified to consider 3D heat transfer model as well as the different pyrolysis reactions involved in the three-steps thermal decomposition model as follows [21-22]:

$$\frac{\partial\left[\left(\rho_{A1}+\rho_{A2}+\rho_{A3}\right)Cp_w+\rho_c Cp_c+\rho_l Cp_l\right]}{\partial t} = \frac{\partial}{\partial x}\left[\lambda_x.\frac{\partial T}{\partial x}\right]+\frac{\partial}{\partial y}\left[\lambda_y.\frac{\partial T}{\partial y}\right]+\frac{\partial}{\partial z}\left[\lambda_z.\frac{\partial T}{\partial z}\right]+Q_r^{"} \quad (5)$$

By introducing the mass fractions of the pseudo-components A_1, A_2, and A_3, the Eq. (5) becomes:

$$\frac{\partial\left[\left(\alpha_1+\alpha_2+\alpha_3\right)\rho_w Cp_w+\rho_c Cp_c+\rho_l Cp_l\right]}{\partial t} = \frac{\partial}{\partial x}\left[\lambda_x.\frac{\partial T}{\partial x}\right]+\frac{\partial}{\partial y}\left[\lambda_y.\frac{\partial T}{\partial y}\right]+\frac{\partial}{\partial z}\left[\lambda_z.\frac{\partial T}{\partial z}\right]+Q_r^{"} \quad (6)$$

where $Q_r^{"}$ is the energy source resulting from the sum of reaction heat of the three pyrolysis reactions (endothermic and exothermic), including the drying at temperature T, which can be expressed as:

$$\begin{aligned} Q_r^{"} &= k_v.\rho_l.\left[\Delta h_o^v+\left(Cp_v-Cp_l\right).\left(T-T_0\right)\right] \\ &+k_1.\rho_{A1}.\left[\Delta h_o^1+\left(Cp_G-Cp_w\right).\left(T-T_0\right)\right] \\ &+k_2.\rho_{A2}.\left[\Delta h_o^2+\left(Cp_G-Cp_w\right).\left(T-T_0\right)\right] \\ &+k_3.\rho_{A3}.\left[\Delta h_o^3+\left(Cp_G-Cp_w\right).\left(T-T_0\right)\right] \end{aligned} \quad (7)$$

Cp_G=2.4, Cp_C=1.39, Cp_l=4.18, Cpv=1.58 (kJ.kg^{-1}.K^{-1}) are the specifc heat for gas, char, liquid, and vapor [20]. Specific heat values, Cp_w, for both compressed and uncompressed wood are taken from experiment of thermogravimetric test at 60 oC (1382 and 1405). Δhi (kJ.kg^{-1}) represent constants of the standard resulting heat for resultants and reactants per unit mass (enthalpy) and they are taken from [20] as follows: $\Delta h_1^0 = \Delta h_2^0 = \Delta h_3^0 = -420$ (for pyrolysis reactions: transformation of wood to char and gas), $\Delta h_v^0 = -2440$ (for drying process: transformation of moisture to vapor).

λ_x, $\lambda_y = \lambda_z$ are the variable thermal conductivity coefficients,

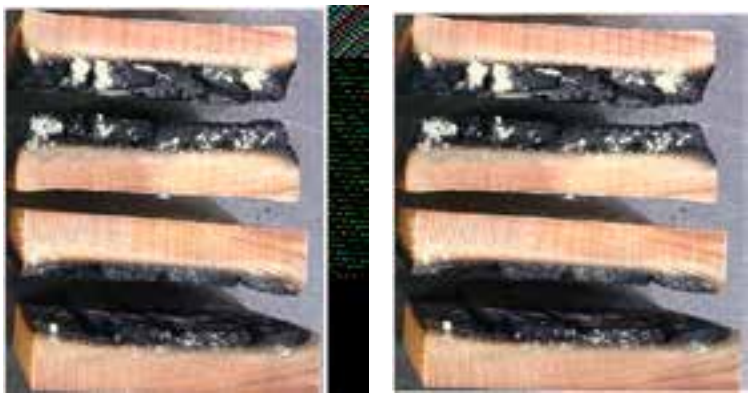

(a) Uncompressed spruce (b) Compressed spruce

Figure 5: Experimental charring layer under 20 kW/m² and 20 min exposure

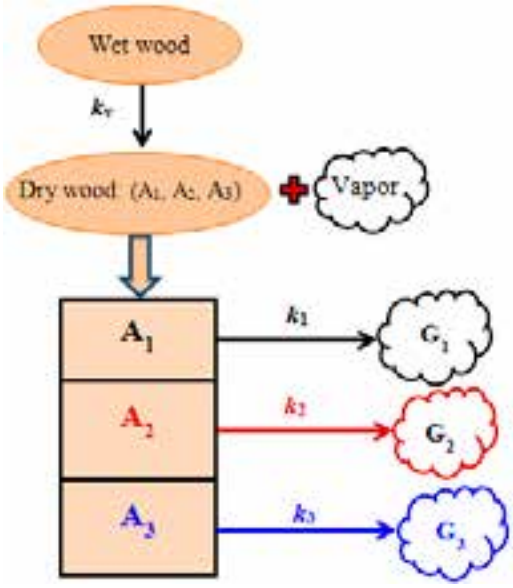

Figure 6: The three-steps multi-reactions of pyrolysis of wet wood

in the transverse and longitudinal directions, of the equivalent solid depending on the solid conversion η and on the thermal conductivity coefficients of char, λ_c, and wet wood λ_w [20]:

$$\lambda_i = \eta.\lambda_{ci} + (1-\eta).\lambda_{wi} \quad (8)$$

$$\lambda_c = 0,07 \quad (9)$$

$$\eta = \frac{\rho_c}{\rho_c + \rho_w} \quad (10)$$

Conductivity reference values for compressed and uncompressed wood are taken from hot plate method (λ_w=0,096 for native wood and λ_w=0,175 for compressed wood), and assumed to evolve as a function of the humidity according to the relation by [20]: λ_w=0.096+0.369X and λ_w=0.175+0.369X, respectively, for uncompressed and compressed wood. X represents the moisture content (in %). Here, the thermal conductivity of wood in the two transverse directions, namely tangential and radial directions, is assumed identical (λ_x=λ_y). While the longitudinal thermal conductivity is assumed to be the same (λ_z=0.2W/(m.K)) as for native wood (uncompressed).

The rate constants of reactions k_1, k_2, and k_3 are assumed to obey the first-order Arrhenius law, depending on the temperature T, the activation energy Ei (J.mol^{-1}) of reaction i, the gas constant R=8.314 J/(mol.K) and the pre-exponent factor Ai (s^{-1}) of the reaction i, as follows:

$$k_i = A_i.\exp\left(\frac{E_i}{RT}\right) \quad (11)$$

Table 1: Identified kinetic parameters for the three-steps pyrolysis model

Reaction	E_i [kJ/mol]	A_i [1/s]	α_i
(1)	102	1,15×10^7	0,25
(2)	220,9	1,16×10^{16}	0,37
(3)	30	5,85×10^{-1}	0,2

The parameters related to fractions α_1, α_2, α_3, the activation energy E_i and the pre-exponent Ai are obtained using the inverse approach based on the mass loss curves and their derivatives obtained from the TGA-type tests. The identified parameter values are summarized in Table 1.

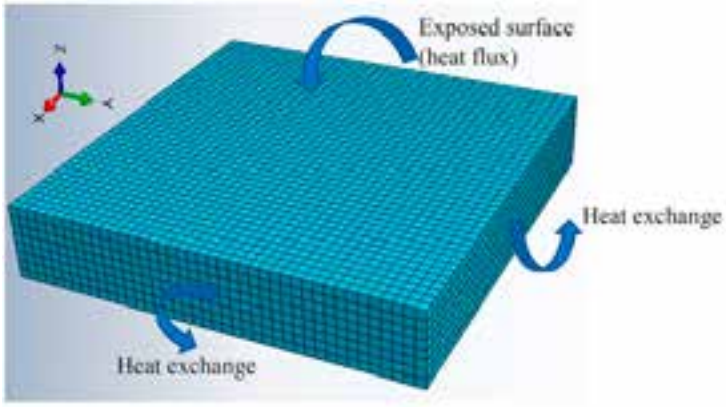

Figure 7: Finite element model of the spruce plate

The developed three-steps pyrolysis reactions finite element model was successfully implemented in the Abaqus commercial software via the user-defined UMATHT.

3.2. Numerical simulation and validation of the FE model

Both uncompressed and compressed spruce square plates were simulated using the developed finite element model. 3D solid quadratic elements of Abaqus (CD320) were used to generate the finite element mesh (Figure 7). It is worth noting that even if the FE-model is a 3D formulation, at this stage of the study the application considered is a one-dimensional problem. Heat exchange, by radiation and convection, was used for the unexposed surfaces to allow exchange with the temperature room (23°C). A heat transfer coefficient of 12.5W/m^2.K and radiative transfer coefficient of 0.92 was used in the simulations.

The thermal profiles for both uncompressed and compressed spruce plates were simulated and compared to the experimentally recorded temperatures (Figure 8). In addition, the Eurocode 5 [23] model was applied for comparison purposes using the surface temperature recorded experimentally on the sample exposed surface (see Figures 3 and 4) as the boundary condition (the imposed temperature). This is similar to the ISO-834 fire curve [24] suggested by the Eurocode. Modified thermo-physical

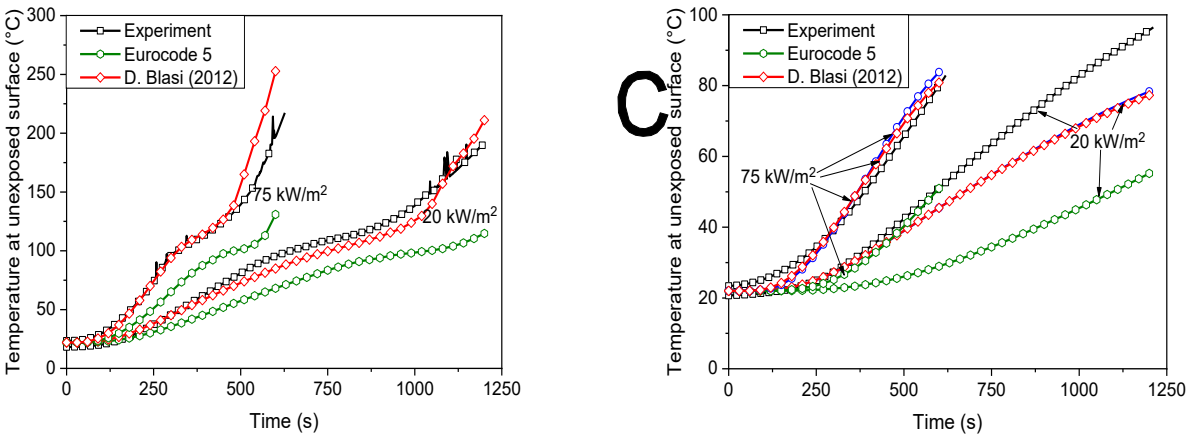

(a) Uncompressed samples

(b) Compressed samples

Figure 8: Temperature profiles at the unexposed surface

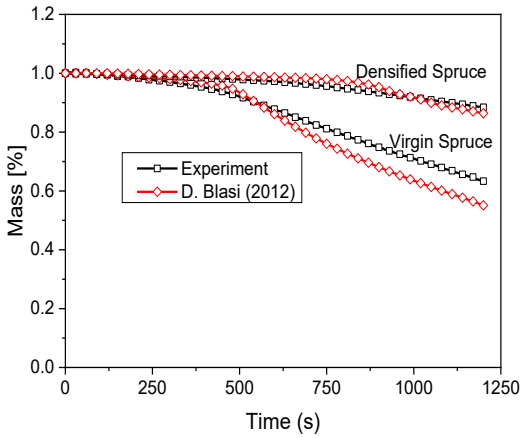

(a) Heat flux of 20 kW/m^2

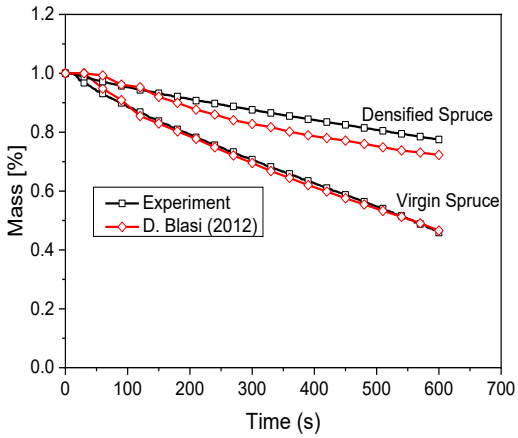

(b) Heat flux of 75 kW/m^2

Figure 9: Comparison of mass loss

(xem tiếp trang 66)

References

1. *L.A. Lowden, T.R. Hull, Flammability behavior of wood and review of the methods for its reduction, Fire Sci. Rev. 2 (2013) 4. http://www.fresciencereviews. com/content/2/1/4.*
2. *Osorio, Andres F., Hidalgo, Juan P., and Evans, Philip D. (2018). Enhancing the fire performance of engineered mass timber and its implications to the fire safety strategy. 2018 World Conference on Timber Engineering, WCTE 2018, Seoul, Korea, August 20-23, 2018. World Conference on Timber Engineering (WCTE).*
3. *W. Gan, C. Chen, Z. Wang, J. Song, Y. Kuang, S. He, R. Mi, P. B. Sunderl and L. Hu, Dense. Self-Formed Char Layer Enables a Fire-Retardant Wood Structural Material Advanced Functional Materials https://doi.org/10.1002/adfm.201807444.*
4. *K. Yue, J. Wu, L. Xu, Z. Tang, Z. Chen, W. Liu, L. Wang. Use impregnation and densification to improve mechanical properties and combustion performance of Chinese fr, Constr. Build. Mater. 241 (2020), 118101.*
5. *G. Chen, C. Chen, Y. Pei, S. He, Y. Liu, B. Jiang, M. Jiao, W. Gan, D. Liu, B. Yang, L. Hu. A strong, flame-retardant, and thermally insulating wood laminate, Chem. Eng. J. 383 (2020), 123109.*
6. *F. Richter and G. Rein. The Role of Heat Transfer Limitations in Polymer Pyrolysis at the Microscale, Front. Mech. Eng. 4:18.doi: 10.3389/fmech.2018.00018.*
7. *I. Vermesi, M. J. DiDomizio, F. Richter, E. J. Weckman, G. Rein. Pyrolysis and spontaneous ignition of wood under transient irradiation: Experiments and a-priori predictions, Fire Safety Journal (In press), https://doi.org/10.1016/j.fresaf.2017.03.081.*
8. *F. Richter, G. Rein, A multiscale model of wood pyrolysis in fire to study the roles of chemistry and heat transfer at the mesoscale, Combust. Flame 216 (2020) 316–325.*
9. *M.J. Antal, G. Varhegyi, E. Jakab. Cellulose pyrolysis kinetics: revisited, Ind. Eng. Chem. Res. 37 (1998) 1268–1275, https://doi.org/10.1021/ie970144v.*
10. *B. Peters, C. Bruch. Drying and pyrolysis of wood particles: experiments and simulation, J. Anal. Appl. Pyrol. 70 (2003) 233–250.*
11. *Lautenberger, Chris, and Fernandez-Pello, Carlos. A model for the oxidative pyrolysis of wood. United States: N. p., 2009. Web. doi:10.1016/J. COMBUSTFLAME. 2009.04.001.*
12. *S.R. Wasan, P. Rauwoens, J. Vierendeels, B. Merci. Application of a simple enthalpy-based pyrolysis model in numerical simulations of pyrolysis of charring materials, Fire Mater. Int. J. (2009), https://doi.org/10.1002/fam.1010.*
13. *P. Patel, T. R. Hull, A. A. Stec and R. E. Lyon. Influence of Physical Properties on Polymer Flammability in the Cone Calorimeter, Polymers for Advanced Technologies 22(7):1100–1107.*
14. *D. Cancellieri, V. Leroy-Cancellieri, E. Leoni, A. Simeoni. Kinetic study of thermal degradation of peats by TGA, VI International Conference on Forest Fire Research.*
15. *Bilbao R, Mastral JF, Ceamanous J, Aldea ME. Modeling of the pyrolysis of wetwood, J Anal Appl Pyrol. 1996; 36; pp.81–97.*
16. *B. Moghtaderi. The state-of-the-art in pyrolysis modeling of lignocellulosic solid fuels, Fire Mater 2006;30:1–34.*
17. *Broström M., Nordina A., Pommer L., Branca C., Di Blasi C. Influence of torrefaction on the devolatilization and oxidation kinetics of wood, Journal of Analytical and Applied Pyrolysis 96 (2012) 100-109.*
18. *I. El-Houjeyri, V.-D. Thi, M. Oudjene, M. Khelifa, A. Sotato, Z. Guan. Experimental investigations on adhesive free laminated oak timber beams and timber-to-timber joints assembled using thermo-mechanically compressed wood dowels, Constr. Build. Mater. 222 (2019) 288–299.*
19. *Terrei L., Acem Z., Lardet P., Georges V., Boulet P., Parent G.. Experimental tools applied to the ignition study of spruce wood under cone calorimeter, Journal of Physics: Conference series volume 1107.*
20. *D.K. Shen, M.X. Fang, Z.Y. Luo, K.F. Cen. Modeling pyrolysis of wet wood under external heat flux, Fire Saf. J. 42 (2007) 210–217.*
21. *V.D. Thi, M. Khelif, M. Oudjene, M. El Ganaoui, Y. Rogaume. Finite element analysis of heat transfer through timber elements exposed to fire, Eng. Struct. 143 (2017) 11–21.*
22. *V.D. Thi, M. Khelifa, M. Oudjene, M. El Ganaoui, Y. Rogaume. Numerical simulation of fire integrity resistance of full-scale gypsum-faced cross-laminated timber wall, Int. J. Therm. Sci. 132 (2018) 96–103.*
23. *EN 1995-1-1:2004. Eurocode 5: design of timber structures – part 1. 1: general rules and rules for buildings, European Committee for Standardization, Brussels Belgium, (E).*
24. *ISO 834-1. Fire-resistance tests. Elements of building construction. Part 1: General requirements. International Organization for Standardization, Geneva, Switzerland; 1999.*